Calculation of vibrational lifetimes in amorphous silicon using molecular dynamics simulations

S. R. Bickham and J. L. Feldman
Complex Systems Theory Branch, Naval Research Laboratory, Washington, DC 20375
(Received 6 January 1998)

The decay of normal-mode excitations is calculated for amorphous silicon through molecular-dynamics simulations within periodic supercells consisting of 216 and 4096 atoms. Phenomenological structural and interatomic potential models are employed. At moderate temperatures, lifetimes are found to be on the order of 10 ps and lifetimes of localized and extended nonpropagating modes are comparable. These features are in agreement with related perturbation theory calculations, and in strong disagreement with the frustrated anharmonic decay predicted by the fracton model and apparently with the results of anti-Stokes Raman experiments performed at $T=10$ K. [S0163-1829(98)01319-8]

The investigation of the vibrational properties of amorphous solids has been an active area of research since Zeller and Pohl first found evidence that the thermal properties of these materials differ remarkably from their crystalline counterparts at low temperatures.[1] In addition, the heat capacities and thermal conductivities of a wide variety of amorphous materials have been found to have the same qualitative and quantitative temperature dependences, indicating an apparent universality. A phenomenological model based on tunneling between states of constant spectral density has been used to explain this behavior. However, the physical nature of these entities is not well understood.[2–4]

To further complicate this picture, recent theoretical[5] and time-resolved Raman[6] studies of the lifetime of high-energy vibrational modes in amorphous silicon disagree by several orders of magnitude. The experimental results were obtained by measuring the decay rates of nonequilibrium phonon populations produced by the relaxation of hot charge carriers following pulsed laser excitation. The temporal evolution of the Stokes and anti-Stokes Raman intensities suggests that the vibrational lifetime increases with increasing frequency and is on the order of 10 ns for the highest-frequency modes. The perturbative study by Fabian and Allen,[5] on the other hand, predicts a ps time scale that follows the two phonon density of states.

A theoretical treatment based on a fractal network, albeit of fractal dimensionality three, has been proposed by Orbach and Jagannathan to explain the experimental results.[7] In their theory of fractons, a crossover length scale is defined that divides the density of states into a (lower frequency) Euclidean form and a (higher frequency) fracton form. The crossover wavelength for amorphous silicon is assumed to be 20 or 30 Å, which corresponds to a low-frequency boundary (mobility edge) between localized and extended states — much lower than for our models that show a quite clear mobility edge near the top of the vibrational spectrum. Of course, we cannot rule out unusual localization on a larger length scale than that of our supercells, which are at most 43 Å along an edge. The work of Fabian and Allen and of Fabian[8] also give contrary evidence to a claim by Orbach and Jagannathan that these localized modes cannot decay as fast as extended phononlike modes.

Here we present the results of calculations of vibrational lifetimes for models of amorphous silicon using molecular-dynamics (MD) simulations. These types of numerical experiments have been increasingly used to study the properties of amorphous materials in an attempt to bridge the gap between theory and experiments. Most recently, they have been used to investigate the Raman spectrum of amorphous silicon[9] and high-frequency modes in fused silica.[10] Although the use of atomistic models restricts the interpretation to the classical regime, experimentally relevant information about the amorphous structure and vibrational modes has been obtained. An early study similar to ours, but for a crystalline model, was done by Dickey and Paskin.[11]

We choose the same potential and structural models as used by Fabian and Allen in their study except that we also make use of a 4096 atom model in addition to their 216 atom model. The 4096 atom model that we use was obtained from Wooten and co-workers[12] and relaxed, as for the 216 atom model, using the Stillinger-Weber (SW) potential.[13] The continuous random network models, like those produced by the Wooten-Winer-Weaire procedure, give radial distribution functions that are in good agreement with the experiment and are also supported by recent ''variable coherence transmission electron microscopy'' experiments in amorphous germanium.[14] Equilibration of those models with respect to the SW potential does not affect the structural characteristics greatly.

The SW potential gives reasonably accurate results for harmonic and quasiharmonic properties of the crystal.[15] The potential's empirical content was structural data from both solid and liquid silicon, the melting temperature of the crystal, and the cohesive energy of the solid. It is important to point out that the SW potential has been shown to yield differences in elastic properties between amorphous and crystalline silicon quite accurately.[16] For a detailed comparison of the SW potential with experiment for mode Grüneisen parameters and pressure dependences of elastic constants see Porter *et al.*[17] and Feldman *et al.*,[18] respectively. The SW potential yields the high-temperature thermal expansivity extremely accurately[17,19] but it has been pointed out[17] that this is due in large part to a cancellation of errors in mode Grüneisen parameters. Recall that Grüneisen parameters depend on third-order derivatives linearly, whereas inverse lifetimes depend on them quadratically (in lowest-order perturbation

theory). Since certain mode Grüneisen parameters are poorly given by the SW parameter and since SW pressure derivatives of elastic constants are too small by about 25% or more, it is not surprising that the crystalline value of the SW inverse lifetime for the TO zone-center mode was found to be too small by a factor of 2 (Ref. 5) in comparison to experiment. A parametrized fit of a generalized Keating cubic-anharmonic model to first principles local-density approximation (LDA) calculations yielded similar disagreement with experiment,[20] but *ab initio* LDA calculations,[21] as well as early empirical tight-binding MD calculations,[22] yielded excellent agreement with experiment. It was suggested in Ref. 20 that their disagreement with experiment was an indication of the need to include anharmonicity to higher-order terms than cubic ones. Finally, we remark that the SW potential cannot represent the observed flattening of acoustic branch dispersion curves or the observed negative thermal expansivity over a low-temperature range.

The 216 atom model is identical to the one used by Fabian and Allen, so the MD and perturbative results are expected to be similar; however, the computer simulations allow the full anharmonic potential to be explored. Decay mechanisms in addition to those due to cubic anharmonicity may therefore contribute to the relaxation. Although the MD results are only applicable to the classical regime, these realistic models for the potential and amorphous structure should yield an order of magnitude estimate of the vibrational lifetime. In addition, we obtain very similar results for supercells with 216 and 4096 atoms, so the finite system size in these calculations does not seem to be a factor. These are the first studies of this nature for a large-scale realistic amorphous system.

Our initial systems are 216 and 4096 atom supercells that have been relaxed to zero temperature and pressure using an incremental time step of $\delta t = 0.005\tau$, where the basic time unit τ is equal to 0.076634 ps. The 216 atom model and a similar one with 1000 atoms have previously been used to calculate the phase diagram[23] and thermal conductivity.[24] Isokinetic ensembles are then obtained by assigning random velocities to each atom and scaling them to correspond to the desired temperature. During a preliminary simulation, these velocities are rescaled at increasing time intervals, which calibrates the kinetic energy of the system without a resonant accumulation of energy in any vibrational modes.[25] After 5000 time steps, the thermostat is removed and the system allowed to adjust to a microcanonical ensemble by continuing the MD simulation for another 50 000 time steps. The instantaneous displacements, velocities, and accelerations are then used as initial conditions in the computer experiments.

At each temperature, kinetic energy is put into selected modes of vibration and monitored as a function of time. Assuming the system is a microcanonical ensemble before the perturbation, the average vibrational energy should be the same in each mode. However, the instantaneous potential and kinetic energies generally differ from the ensemble average, which complicates the comparison of the decay rates for different modes and/or different temperatures. To eliminate this problem, we found it useful to remove the initial potential and kinetic energy in the desired mode before adding the perturbation. This condition, which fixes the initial phase and amplitude of the vibrational mode, may be expressed as

$$\vec{\mathbf{r}} = \vec{\mathbf{r}}_{\mathbf{T}} - \{\hat{\mathbf{e}}(\omega_0)\cdot[\vec{\mathbf{r}}_{\mathbf{T}} - \vec{\mathbf{r}}_0]\}\hat{\mathbf{e}}(\omega_0) \tag{1}$$

and

$$\vec{\mathbf{v}} = \vec{\mathbf{v}}_{\mathbf{T}} - [\hat{\mathbf{e}}(\omega_0)\cdot\vec{\mathbf{v}}_{\mathbf{T}}]\hat{\mathbf{e}}(\omega_0) + A_0\omega_0\hat{\mathbf{e}}(\omega_0), \tag{2}$$

where $\vec{\mathbf{r}}_{\mathbf{T}}$ and $\vec{\mathbf{v}}_{\mathbf{T}}$ are $3N$-dimensional vectors that represent the instantaneous displacements and velocities at temperature T, $\vec{\mathbf{r}}_{\mathbf{0}}$ are the equilibrium coordinates at zero temperature, and A_0 is the scaling amplitude for the energy put into a vibrational mode with eigenvector $\hat{\mathbf{e}}(\omega_0)$ and frequency ω_0. Strictly speaking, Eqs. (1) and (2) are appropriate if the eigenvectors are independent of temperature. We find that this is indeed the case for temperatures below 30 K, but the average displacements and zero-temperature coordinates deviate at higher temperatures as the system accesses other configurations during the constant volume simulations. Some of the high-frequency modes are strongly affected by these structural changes since they are spatially localized with dynamics that depend on the local environment.

After the perturbation described above, the kinetic energy in a given mode is monitored as a function of time by computing

$$K(\omega_0,t) = [\hat{\mathbf{e}}(\omega_0)\cdot\vec{\mathbf{v}}]^2. \tag{3}$$

The instantaneous kinetic energy is a rapidly oscillating function, so $K(\omega_0,t)$ is averaged over a few vibrational periods to smooth the data. This type of probe is valid as long as the decay rate is slow compared to the vibrational period, which is the case for the modes and temperatures considered here. To check that the system has actually reached equilibrium, the power spectral density (PSD) of the lattice is computed to monitor changes in the nonequilibrium density of states. The PSD has the advantage of not requiring the normal-mode eigenvectors, however, direct calculation of the kinetic energy using Eq. (3) yields information on specific modes rather than the average of a group of modes that lies within a small frequency band.

In the weak perturbation limit, the kinetic energy of the mode is assumed to decay exponentially, in which case the atomic velocities have the time dependence

$$v_{\alpha,i} = e_{\alpha,i}A_0\omega_0 e^{-t/\tau}\cos(\omega_0 t). \tag{4}$$

The equilibrium value at $t=\infty$ has been neglected in this analysis, but it should be noted that the kinetic energy in each mode decays to a equilibrium value of $kT/2$, not zero. Inclusion of this term does not significantly affect the calculated value of the decay rate, so it will not be considered further. With this approximation, the average kinetic energy during one vibrational period τ_0 is then

$$\langle K(\omega_0)\rangle = \frac{A_0^2\omega_0^2\tau}{4\tau_0}(1-e^{-2t_0/\tau}). \tag{5}$$

The lifetime of the mode is then $\tau/2$, and the corresponding decay rate is $\Gamma = 2\hbar/\tau$.

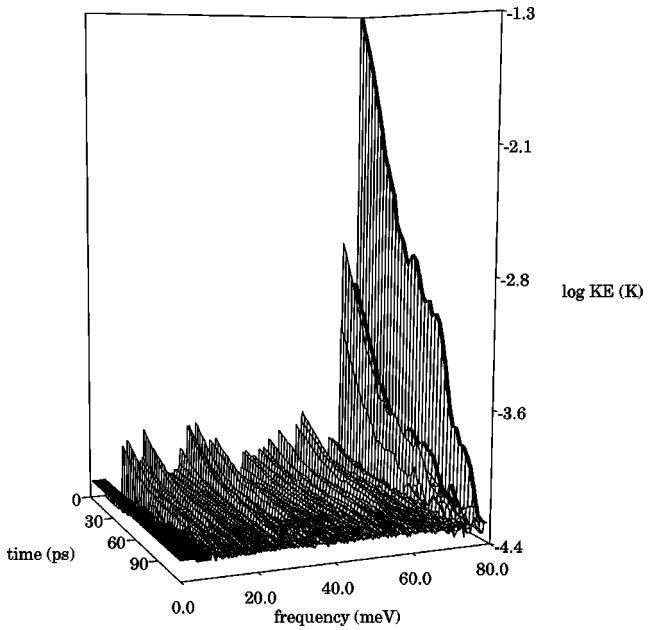

FIG. 1. Logarithm (base 10) of the average kinetic energy as a function of time and frequency for the initial conditions described in the text. The kinetic energy is averaged over successive time intervals of 3.1 ps for each of the 648 modes during a 122.6 ps simulation.

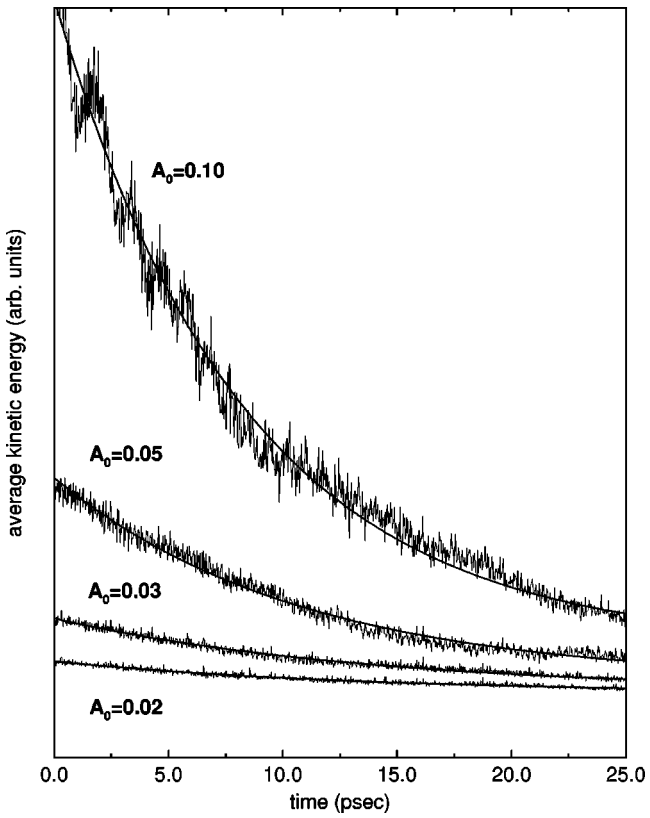

FIG. 2. Exponential fits to the average kinetic energy of the highest-frequency mode in the 4096 atom supercell for different perturbation amplitudes. The initial temperature is 5 K and the vibrational frequency is 87.8 meV. The oscillations in the $A_0=0.10$ curve are due to anharmonic coupling to other localized modes. The lifetime increases with decreasing perturbation amplitude and extrapolates to a value of approximately 14 ps at $A_0=0$.

Energies have been calculated using Eq. (3) for a perturbation with amplitude $A_0=0.05$ in the highest-frequency mode in the 216 atom supercell with $\omega_0=78.7$ meV. This produces a net temperature increase of 4 K from the initial temperature of 5 K. The log kinetic energies of all 648 modes are plotted as a function of time and frequency in Fig. 1. The data are obtained by averaging Eq. (3) over 3.1 ps intervals for each vibrational frequency, and the maxima of the time and frequency axes are 122.6 ps and 78.7 meV, respectively. Although the perturbation energy is put into a single mode, a small portion is quickly and nonradiatively transferred to other modes by anharmonic coupling. The initial kinetic energy spectrum therefore has a strong peak at the perturbation frequency with secondary peaks at lower frequencies. As the simulation progresses, this nonequilibrium distribution evolves into a microcanonical ensemble with each mode having the same average kinetic energy. The time scale for this relaxation is on the order of tens of ps, and similar decay times have been obtained for other localized and extended, nonpropagating modes in the 216 atom model.[26]

In the derivation of Eq. (4), the amplitude in a given mode is assumed to decay exponentially as the system evolves towards equilibrium. This implies that the lifetime is independent of the perturbation amplitude. Figure 2 shows the decay of the kinetic energy of a localized mode with a frequency of 87.8 meV in the 4096 atom system for four different perturbation amplitudes. The initial temperature of 5 K increased by 1.05, 0.28, 0.11, and 0.06 K for input amplitudes of $A_0=0.10$, 0.05, 0.03, and 0.02, respectively. Exponential fits to the simulation data are plotted with heavy lines, yielding lifetimes of 8.3, 11.7, 13.9, and 13.9 ps, respectively. This functional form is an excellent fit for all four cases, although low-frequency oscillations in the average kinetic energy are evident when the perturbation amplitude is large. A more detailed analysis shows that these oscillations arise from coupling to other high-frequency localized modes. Although these modes are orthogonal in the harmonic limit, they are not always spatially isolated and may be coupled by anharmonicity when nearest or next-nearest neighbors are shared. This coupling does not, however, appear to be a significant decay mechanism. The small amplitude lifetime is approximately 14 ps, which is in qualitative agreement with the lifetimes of other modes in the 216 and 4096 atom supercells.

The temperature dependence of the decay rates is obtained by extrapolating lifetimes such as those determined from the simulation data in Fig. 2 to the limit of zero perturbation amplitude. The perturbative decay rates for the highest-frequency mode in the 216 atom supercell are plotted by the dashed curve in Fig. 3, while the MD results for the same mode are plotted using open squares. The error bars are representative of the uncertainty in the numerical fits due to finite simulation times, statistical noise, and the background kinetic energy level. The solid line represents the best linear fit to the simulation data. Note that the MD decay rate is approximately a factor of 2 larger than the high-temperature limit of the perturbative result, which indicates that higher orders of anharmonicity not included in the latter analysis may be important. The MD decay rates for the highest-

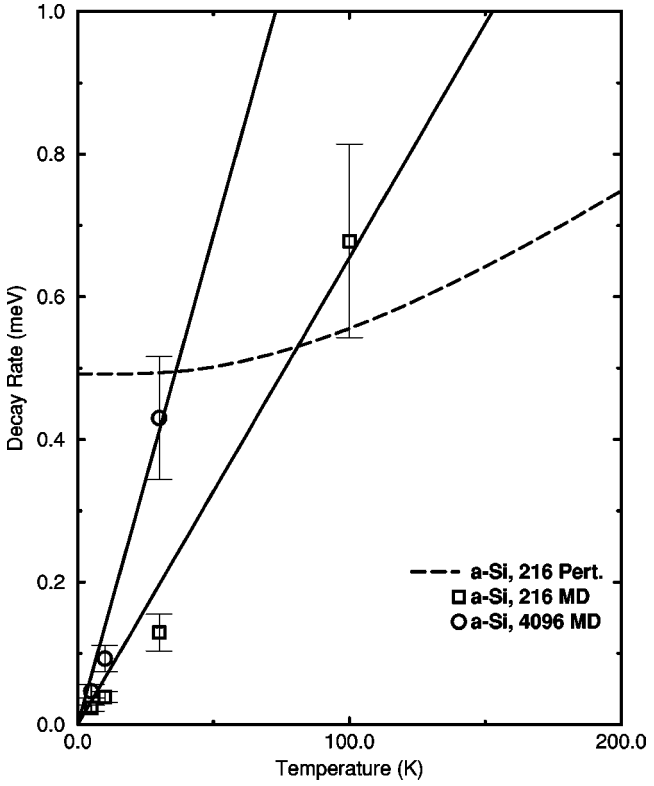

FIG. 3. Log decay rates as a function of temperature for modes in amorphous silicon. The perturbative and MD decay rates for the highest-frequency mode in the 216 atom supercell of *a*-Si are plotted with the dashed curve and open squares, respectively, while the open circles represent the MD decay rate for the highest-frequency mode in the 4096 atom supercell.

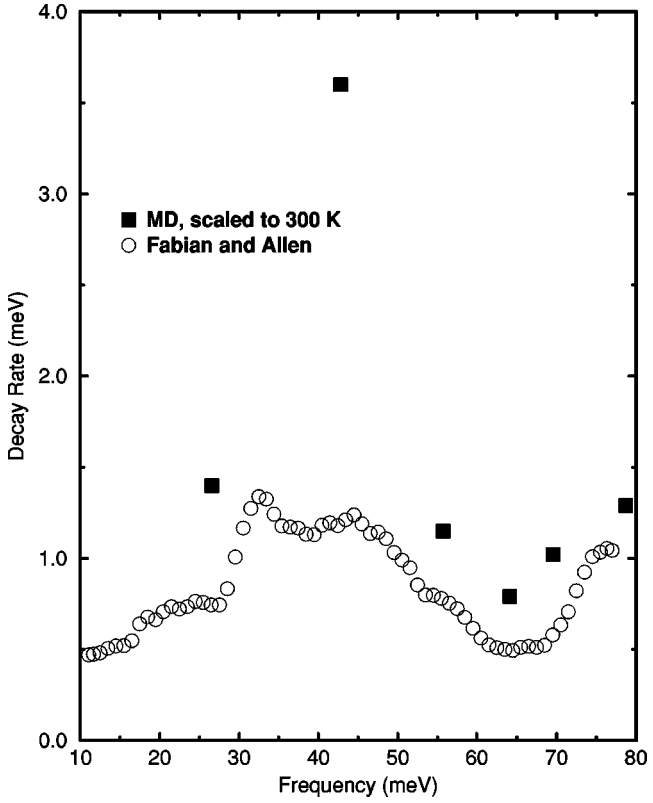

FIG. 4. Frequency dependence of decay rates in the 216 atom supercell of amorphous silicon. Solid squares represent simulation results at 5 and 10 K that have been scaled to 300 K and averaged. The perturbative results of Fabian and Allen are plotted using open circles.

frequency mode in the 4096 atom supercell are plotted using open circles, with the best linear fit represented by the solid line. The slope is larger than that for the highest-frequency mode in the 216 atom model; however, it is important to note that these modes are idiosyncratic, with decay rates that strongly depend on their local environments. For example, the modes in the 216 atom model with the highest six frequencies are all strongly localized with similar inverse participation ratios, but have decay rates (lifetimes) that range from 0.02 to 0.04 meV (30–15 ps) at 5 K.

The decay rates for several modes in the 216 atom model are plotted as a function of frequency in Fig. 4. The simulation results for initial temperatures of 5 and 10 K have been averaged, scaled to 300 K, and plotted using solid squares. The scaling was done under the assumption that the decay rates scale linearly with temperature, which would be the case if there were only cubic anharmonicity. This is a good approximation for small amplitude perturbations in the Stillinger-Weber potential, but the actual temperature dependence is actually sublinear due to higher orders of anharmonicity. For comparison, the perturbative results of Fabian and Allen are plotted using open circles.[5] There is good qualitative and quantitative agreement over the entire frequency range except near 40 meV where there is a minimum in the density of states.[24] The width assigned to the δ functions in the perturbative analysis could affect the calculated decay rates in this region since there are relatively few modes in each bin. Note that the MD decay rates are always faster since all orders of anharmonicity contribute to the vibrational relaxation.

In summary, molecular-dynamics simulations have been used to calculate vibrational lifetimes in realistic models of amorphous silicon. These are the first calculations of this nature for large amorphous supercells and demonstrate the ability to extract experimentally relevant information from computer simulations. The lifetimes found by this method are in good agreement with the perturbative calculations of Fabian and Allen and are on the order of 10 ps at low temperatures in both 216 and 4096 atom supercells. The lifetimes of high-frequency localized modes and extended, nonpropagating modes with intermediate frequencies are comparable, in contrast to Raman experiments that find that the lifetime is on the order of 10 ns and increases dramatically with increasing frequency.[6] While this is a significant discrepancy, it is unclear if the experiments and simulations are measuring the same quantities. In the Raman experiments, a large nonequilibrium phonon population was excited over the entire vibrational spectrum, with a typical phonon occupation of 0.2 for the TO mode. This yields a temperature of several hundred degrees in the region of the laser spot. Although this is well below the melting temperature, there will be local structural rearrangements as the system relaxes to nearby metastable configurations. It is well known that glass dynamics involve fast fluctuations about

local structures as well as time evolution of the nonequilibrium local structures themselves. These latter processes can occur on all time scales, even at low temperatures,[27] and their coupling to normal-mode vibrations should be taken into account. To add more realism to the computer experiments, the decay rates of spatial and temporal energy pulses are being calculated, allowing a more direct simulation of the experimental conditions. An analysis of the amorphous structure of different size models is also being done to examine the influence of temperature-induced changes in the local environment on the vibrational properties

We wish to thank P. B. Allen, J. Fabian, R. Orbach, G. Engel, and J. Q. Broughton for stimulating discussions. We thank M. Kluge for pointing out Ref. 7 to us. One of us (S.R.B.) acknowledges support by the NRC. This work was supported in part by the Office of Naval Research.

[1] R. C. Zeller and R. O. Pohl, Phys. Rev. B **4**, 2029 (1971).
[2] W. A. Phillips; J. Low Temp. Phys. **7**, 351 (1972); Rep. Prog. Phys. **50**, 1657 (1987).
[3] P. W. Anderson, B. Halperin, and S. Varma, Philos. Mag. **25**, 1 (1972).
[4] B. E. White and R. O. Pohl, Phys. Rev. Lett. **75**, 4437 (1995).
[5] J. Fabian and P. B. Allen, Phys. Rev. Lett. **77**, 3839 (1996).
[6] A. J. Scholten and J. I. Dijkhuis, Phys. Rev. B **53**, 3837 (1996); A. J. Scholten, A. V. Akimov, and J. I. Dijkhuis, *ibid.* **47**, 13 910 (1993).
[7] R. Orbach, Philos. Mag. B **65**, 289 (1992); R. Orbach and A. Jagannathan, J. Phys. Chem. **98**, 7411 (1994); R. Orbach (unpublished).
[8] J. Fabian, Phys. Rev. B **55**, R3328 (1997).
[9] M. Marinov and N. Zotov, Phys. Rev. B **55**, 2938 (1997).
[10] B. Guillot and Y. Guissani, Phys. Rev. Lett. **78**, 2401 (1997).
[11] J. M. Dickey and A. Paskin, Phys. Rev. **188**, 1407 (1969).
[12] F. Wooten, K. Winer, and D. Weaire, Phys. Rev. Lett. **54**, 1392 (1985); F. Wooten (private communication); B. R. Djordjevic, M. F. Thorpe, and F. Wooten, Phys. Rev. B **52**, 5685 (1995).
[13] F. H. Stillinger and T. A. Weber, Phys. Rev. B **31**, 5262 (1985).
[14] J. M. Gibson and M. M. J. Treacy, Phys. Rev. Lett. **78**, 1074 (1997).
[15] E. R. Cowley, Phys. Rev. Lett. **60**, 2379 (1988).
[16] M. D. Kluge and J. R. Ray, Phys. Rev. B **37**, 4132 (1988).
[17] L. J. Porter, J. F. Justo, and S. Yip, J. Appl. Phys. **82**, 5378 (1997).
[18] J. L. Feldman, J. Q. Broughton, and F. Wooten, Phys. Rev. B **43**, 2152 (1991).
[19] J. C. Noya, C. P. Herrero, and R. Ramirez, Phys. Rev. B **53**, 9869 (1996).
[20] S. Narasimhan and D. Vanderbilt, Phys. Rev. B **43**, 4541 (1991).
[21] A. Debernardi, S. Baroni, and E. Molinari, Phys. Rev. Lett. **75**, 1819 (1995).
[22] C. Z. Wang, C. T. Chan, and K. M. Ho, Phys. Rev. B **40**, 3390 (1989).
[23] J. Q. Broughton and X. P. Li, Phys. Rev. B **35**, 9120 (1987).
[24] J. L. Feldman, M. D. Kluge, P. B. Allen, and F. Wooten, Phys. Rev. B **48**, 12 589 (1993).
[25] S. R. Nagel, A. Rahman, and G. S. Grest, Phys. Rev. Lett. **47**, 1665 (1981).
[26] S. R. Bickham and J. L. Feldman, Philos. Mag. B **77**, 513 (1998).
[27] L. R. Narasimhan, K. A. Littau, D. W. Pack, Y. S. Bai, A. Elschner, and M. D. Fayer, Chem. Rev. **90**, 439 (1990).